Electronic Supplementary Material (ESI) for Chemical Communications.

A potential catalyst for continuous methane partial oxidation to methanol using N_2O: Cu-SSZ-39

Ozgun Memioglu, Bahar Ipek*

Department of Chemical Engineering, Middle East Technical University, Ankara, 06800, Turkey.
E-mail: bipek@metu.edu.tr

SUPPORTING INFORMATION

S1. Materials and Methods

S1.1. Zeolite Synthesis

SSZ-13: SSZ-13 was hydrothermally synthesized using a gel mixture having a molar composition of $1SiO_2$:$0.035Al_2O_3$:0.5TMAdaOH:$20H_2O$ in the absence of Na^+ ions. In the synthesis, 26.969 g of *N,N,N*-trimethyl-1-adamantanamonium hydroxide solution (TMAdaOH, Sachem, 20 wt.%) as structure directing agent and 0.597 g aluminum ethoxide (Sigma Aldrich, 97wt.%) as Al- source were stirred for 15 minutes at room temperature to dissolve the aluminum ethoxide. After that, 10.850 g tetraethyl orthosilicate (TEOS, Merck, 98 wt.%) were added to the mixture as silicon source and stirred for 1 hour at 298 K. The resulting mixture was transferred to the 35 mL Teflon-lined autoclaves and subjected to hydrothermal treatment at 423 K for 7 days under autogenous pressure in static oven. Hydrothermally produced crystals were recovered by vacuum filtration, washed with 500 mL de-ionized water and dried at 353 K overnight. Calcination was performed in a flow furnace with 15 cm^3 min^{-1} dry air flow at 853 K for 6 h (using a heating rate of 1 K min^{-1}) following drying at 393 K for 2 h. This sample is denoted as Micro-H-SSZ-13

SSZ-39: Na-SSZ-39 was synthesized hydrothermally using tetramethyl piperidinium hydroxide (Sachem, Inc., 35.3 wt.%) as structure directing agent (SDA) with a gel composition of: $0.25Na_2O$:$0.019Al_2O_3$:$1SiO_2$:0.19SDA:$22H_2O$. 6.690 g of SDA, 17.671 g of de-ionized water, 12.840 g of sodium silicate solution (Merck, 37 wt.% Na_2SiO_3, 26.5 wt.% SiO_2) and 1.026 g 1 M NaOH solution were stirred for 15 minutes at 298 K. After obtaining a clear solution, 1.238 g NH_4-USY (Alfa Aesar, Zeolite Y, Si/Al = 6) was added very slowly to the mixture and the stirring continued for 30 minutes [1]. The synthesis gel was then transferred to 35 mL Teflon-lined autoclaves and hydrothermally treated at 423 K for 7 days under tumbling at 45 rpm. Hydrothermally produced crystals were recovered by vacuum filtration, washed with 500 mL de-ionized water and dried at 353 K overnight. Calcination was performed in a flow furnace under 15 cm^3 min^{-1} dry air flow at 833 K for 8 h (using a heating rate of 1 K min^{-1}) following drying at 393 K for 2 h. The sample is denoted as Micro-Na-SSZ-39.

Omega: The synthesis of MAZ type zeolite (Omega) was performed using a gel composition of $0.24Na_2O$:$0.1Al_2O_3$:$1SiO_2$:0.024TMAOH:$11H_2O$ following a similar procedure given by Gossens et al. [2]. 2.117 g tetramethyl ammonium hydroxide (Merck, 25 wt. %) as the structure directing agent, 11.476 g de-ionized water, 1.020 g NaOH (Merck, 99 wt. %) and 2.242 g sodium aluminate as Al- source were added respectively and stirred for 15 minutes at 298 K. After obtaining a clear solution, 18.144 g of colloidal silica (Ludox HS 40 wt %) was added to the solution as silicon source. Solution was aged for 3 days at room temperature under stirring. The final gel was then transferred to 35 mL Teflon-lined autoclaves and hydrothermally treated at 373 K for 15 days under autogenic pressure and static conditions. Hydrothermally produced crystals were recovered by vacuum filtration, washed with 500 mL de-ionized water and dried at 353 K overnight. Calcination was performed in a flow furnace under 15 cm^3 min^{-1} dry air flow at 823 K for 16 h (using 1 K min^{-1} heating rate) following drying at 393 K for 2 h to remove water and organic species and finally cooled down to the room temperature. The sample is denoted as Na-omega

Mesoporous SSZ-13: Mesoporous SSZ-13 was synthesized using a procedure given by Li et al. [3]. The molar ratios in the gel formula are $1SiO_2$:0.025 Al_2O_3:0.1Na_2O 0.2TMAdaOH:44H_2O:0.12CTABr. First, 38.977 g *N,N,N*-trimethyl-1-adamantanamonium hydroxide (TMAdaOH, Sachem, 20 wt.%), which was employed as the structure directing agent was mixed with 0.979 g sodium hydroxide pellets (NaOH, Merck, 99 wt.%) and 114.879 g de-ionized water until a clear solution was obtained. After that, 11.079 g fumed silica (Sigma Aldrich, 99.8wt.%) as silicon source was added very slowly to the solution and stirred until a homogeneous solution was obtained. Finally, 0.855 g sodium aluminate (Sigma Aldrich, 53wt.% Al_2O_3) as alumina source was added. The gel was stirred for two hours at 298 K to obtain a homogeneous gel. The initial gel was transferred into 35 mL Teflon-lined autoclaves and kept at 433 K for one day. After one day, 1.646 g cetyltrimethylammonium bromide (Sigma Aldrich, 98 wt.%, CTABr) as mesoporogen (SiO_2:CTABr=0.12) was mixed completely with the solution. The final gel that contains CTABr was transferred back into the Teflon-lined autoclaves and hydrothermal treatment was performed at 433 K for 11 more days under static conditions. The sample was collected using vacuum filtration, washed vigorously with de-ionized water and dried at 353 K overnight. The zeolite calcined at 853 K for 10 h in a muffle furnace using a heating rate of 1 K min^{-1} following drying at 393 K for 90 min. The sample is denoted as Meso-Na-SSZ-13.

Mesoporous SSZ-39: Mesoporous SSZ-39 was synthesized using CTABr as mesoporogen. Firstly, 6.690 g tetramethyl piperidinium hydroxide (Sachem, Inc., 35.3 wt.%) was mixed with 17.671 g de-ionized water. After that, 12.840 g sodium silicate solution (Merck, 37 wt.%) as silica source and 1.026 g 1 M NaOH solution was added and stirred for 30 minutes in order to form a homogeneous solution. Afterwards, 1.238 g NH_4-USY (Alfa Aesar, Zeolite Y, Si/Al =6), which was employed as silicon and alumina source was added very slowly to the solution and stirred for 45 minutes. The initial gel was transferred into a 35 mL Teflon-lined autoclaves and kept at 423 K under tumbling at 45 rpm for 1 day and after 1 day, 3.462 g cetyltrimethylammonium bromide (Sigma Aldrich, 98 wt.%, CTABr) as mesoporogen (SiO_2:CTABr=0.12) was mixed with the solution. Final gel containing CTABr was transferred into the Teflon-lined autoclaves again and heated at 423 K for 6 more days under rotation at 45 rpm. The crystals were collected using vacuum filtration, washed vigorously with de-ionized water and dried at 353 K overnight. The zeolite was calcined at 853 K for 16 h using a heating rate of 1 K min^{-1} in a muffle furnace following drying at 393 K for 90 min. The sample is denoted as Meso-Na-SSZ-39.

The ammonium form of Mordenite (NH_4^+-Mordenite, Si/Al=10) was commercially obtained from Alfa-Aesar. The dealumination of NH_4^+-Mordenite was performed using a procedure given by Leng et al. [4]. In the procedure, the first step is acid treatment. 1 g of proton form of the zeolite was stirred in 20 mL 2 M aqueous HNO_3 solution at 373 K for 2 hours. The slurry was vacuum filtrated, washed thoroughly with de-ionized water and the filter cake was calcined at 823 K for 5 hours. In the second step, the sample was refluxed with 0.2 M of NaOH solution, (20 mL solution per gram of zeolite) at 343 K for half an hour. The sample was vacuum filtered and washed with de-ionized water. Finally, the resulting zeolite was refluxed with 0.2 M of HNO_3 solution at 323 K for 1.5 hour. The final product was ammonium-exchanged (three times) and then heat-treated at 823 K for 5 hours to obtain mesoporous H^+-Mordenite.

S1.2. Ion-exchange Procedures

NH_4^+-Exchange: NH_4^+-exchange was performed using 1–3 g of calcined Na^+-zeolite in 500 mL of 0.2 M ammonium nitrate (NH_4NO_3, Sigma Aldrich, 99 wt %,) aqueous solution (500 mL de-ionized water and 8 g NH_4NO_3). The solution was stirred for 3 hours at a temperature of 353 K for exchange. After three hours, zeolites were vacuum filtered using cellulose acetate membrane filters having a pore size of 200 nm, washed with 500 mL de-ionized water and dried at a temperature of 353 K in air for 30 minutes. This exchange procedure was repeated using the same zeolite and a new 0.2 M ammonium nitrate solution for three times. Finally, NH_4^+-exchanged zeolite was heat treated at 823 K for 5 h following drying at 423 K for 1.5 h. Resulting zeolite is denoted as H^+-zeolite (Eq 1).

$$NH_4^+ - zeolite \xrightarrow{\Delta} H^+ - zeolite + NH_3$$

Eq. 1

Cu(II)-Exchange: Copper exchange was performed by exchanging the H^+-form of the zeolites in copper (II) acetate solution at 298 K. 1 g H^+-zeolite was exchanged with Cu(II) in 250 mL of copper (II) acetate·H_2O (Merck, >99 wt.%) solution at room temperature for 6 h to obtain Cu(II)-zeolite. The volume of the solution was kept constant at 250 mL, while the amount of required copper (II) acetate in the solution varied depending on the mass of zeolite and starting Cu/Al ratio (0.35 or 0.70, see Table S1) in the solution. After exchange, resulting Cu(II)-zeolites were filtered, washed with 500 mL de-ionized water and dried at a temperature of 353 K for overnight. Finally, Cu(II)-exchanged zeolites were heat-treated at 723 K for 4 h using a heating rate of 2 K min^{-1} to eliminate any acetate from the zeolites following drying at 423 K for 1 h. Resulting zeolites were denoted as Cu(II)-Zeolite.

Table S1. Cu(II)-exchange details at 298 K for 6 h

Zeolite	Si/Al	Starting Cu(II) concentration (M)	Starting Cu/Al in solution
Micro-H^+-Mordenite	10	0.002	0.35
Meso- H^+-Mordenite	16	0.001	0.35
Micro- H^+-SSZ-13	9	0.002	0.35
Micro- H^+-SSZ-13-2	10	0.004	0.70
Meso- H^+-SSZ-13	16	0.001	0.35
Micro- H^+-SSZ-39	6.3	0.003	0.35
Micro- H^+-SSZ-39-2	7.0	0.005	0.60
Meso- H^+-SSZ-39	15	0.003	0.70
H^+-Omega	3.6	0.004	0.20

S1.3. Characterization Methods

X-ray diffraction data were obtained after calcination of the samples. Powder XRD patterns of calcined zeolites were recorded using a Rigaku Ultima-IV X-ray diffractometer (40 kV, 30 mA) equipped with Cu Kα radiation, (λKα =1.5418 Å) in the 2θ range of 2–50° with a scanning speed of 1 ° min^{-1} at Central Laboratory, METU.

The surface area and pore volume of the samples were determined using N_2 adsorption/desorption isotherms obtained at 77 K. N_2 physisorption isotherms were obtained using a surface area and pore volume analyser; Micromeritics Tristar II 3020 located in the Chemical Engineering Department, METU. The degassing process preceding the N_2 adsorption experiment was performed using Micromeritics VacPrep 061. The samples were previously degassed at 573 K for 6 h under vacuum conditions before N_2 (Oksan, 99.999 %) adsorption. N_2 adsorption/desorption experiment was performed using P/P_0 relative pressure values of N_2 (Oksan, 99.999%) between 10^{-5} and 0.99 and the temperature were kept constant at 77 K using liquid nitrogen. The t-plot method was used to calculate the micropore volume (V_{micro}) of the prepared samples [5]. The mesopore volumes were calculated by subtracting the t-plot micropore volume from the single point pore volume obtained at P/P_0=0.98. Langmuir surface area of the samples were also obtained and presented. The pore size distributions were evaluated using Barret-Joyner-Halenda (BJH) Adsorption model [6].

Morphology of the calcined samples were determined using Scanning Electron Microscopy (SEM) on a QUANTA 400F Field Emission microscope operated at 20 kV. The samples were coated by Pd-Au mixture prior to analysis.

Elemental compositions of samples were determined using inductively coupled plasma-optical emission spectrometer (Perkin Elmer Optime4300DV, ICP-OES) at METU Central Laboratory. The samples were first dissolved with HF/HNO_3 solution overnight. Si, Al and Cu(II) contents of the samples were also determined utilizing Energy Dispersive X-ray spectra (EDX) QUANTA 400F Field Emission SEM at METU Central Laboratory. EDX operated at the voltage of 20 kV by scanning at least 4 different regions.

S1.4. Catalytic Methane to Methanol Conversion Tests

Methane to methanol reaction was conducted in a quartz tubular reactor having 7 mm inner diameter and 9 mm outer diameter. The reactor was mounted on an oven and oven temperature was controlled using a thermocouple wrapped around the quartz reactor near the center of the catalyst bed with Ordel PC771 temperature controller. Zeolite powder was pressed into pellets at a pressure of 60 bar for 4 minutes and sieved into 250–450 μm particle size. Particle size was an important parameter since it would affect both the pressure drop and mass transfer rate. Zeolites were packed between quartz wool plugs in the reactor and placed in the middle of the furnace heating zone. The catalyst bed length was kept approximately 1 cm. The flow rates of gases which are helium (Hatgaz, 99.999% purity), nitrous oxide (Hatgaz, 99%) and methane (Hatgaz, 99.995%) were controlled by separate mass flow controllers (ALICAT, MC-100SSCM-D). Water was introduced into the feed gas stream by directing gas stream to a water bubbler maintained at room temperature that resulted in 2.6 kPa H_2O pressure at 295 K. In order to increase the water partial

pressure, H_2O saturator was heated to 320 K (10.1 kPa at 320 K). All the gas lines are heated at >343 K to prevent any condensation. The effluent stream was directed into a gas chromatograph (GC, Agilent7820A) equipped with a Pora-Plot Q column (CP7554, 25 m, 0.53 mm, 20 µm) and CP- Molsieve 5Å column (CP7538, 25 m, 0.53 mm, 50 µm) with thermal conductivity detector and flame ionization detector. The thermal conductivity and flame ionization detector were used simultaneously in order to detect the products. The qualitative and quantitative analysis of N_2, CO, CO_2, N_2O, CH_4 and dimethyl ether (DME) were performed using single point calibration of a standard gas sample. The methanol calibration was performed by saturating inert He by methanol vapour at 298 K and at 273 K.

Reaction Procedure: Approximately 0.300 g hydrated Cu(II)-zeolites having 250–450 µm particle sizes were placed into the quartz reactor. The total flow rate of the feeding mixture was set to the 100 cm^3 min^{-1}. The feed involved different gas composition of methane, nitrous oxide, water vapour and balance helium. First of all, the sample was purged for 20 min with the feed mixture at room temperature and then a single run was taken in order to determine the initial amounts of reactants. Afterwards, reactor was heated to reaction temperature using a 5 K min^{-1} heating rate and kept at this temperature during the reaction. During the reaction, reaction effluent was sent to the gas chromatograph in 21 min intervals. The first screening of the zeolite activity was performed using a reaction temperature of 573 K with a feed composition of 40 mole % CH_4, 10% N_2O, 3% H_2O and balance He using 100 sccm total flow rate at atmospheric pressure. The rate orders for Micro-Cu-SSZ-39 were performed using a CH_4 partial pressure interval of 20–40 kPa and N_2O partial pressure interval of 5–15 kPa. The activation energy was calculated using the rate information obtained at 543 –598 K.

The conversion, selectivity and TOF values are calculated using equations given below, where F_{CH4} is the molar flow rate of the inlet methane in µmol h^{-1}.

$$X_{CH4}(\%) = \frac{r_{CH4}}{F_{CH4}/g_{cat}} \qquad \text{Eq S1}$$

$$X_{N2O}(\%) = \frac{r_{N2}}{F_{N2O}/g_{cat}} * 100 \qquad \text{Eq S2}$$

$$TOF_{CH4}\left(\frac{mol\ CH_4}{mol\ Cu\ h}\right) = \frac{r_{CH4}}{Cu\ concentration} \qquad \text{Eq S3}$$

$$S_{CH3OH} = \frac{r_{CH3OH}}{r_{CH3OH} + 2 * r_{DME} + r_{CO} + r_{CO2}} * 100 \qquad \text{Eq S4}$$

$$r_{CH4}(\mu mol\ g^{-1} h^{-1}) = r_{CH3OH} + 2 * r_{DME} + r_{CO} + r_{CO2} \qquad \text{Eq S5}$$

S2. Characterization Results

S2.1. Powder XRD Patterns

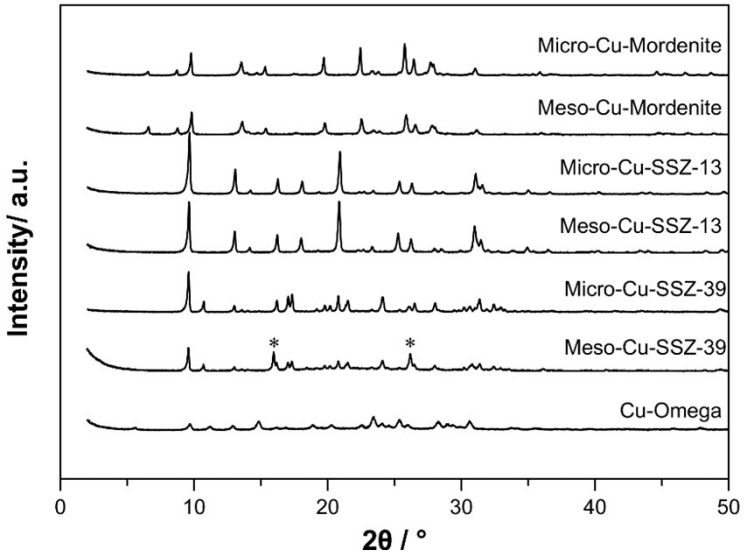

Fig. S1 Powder XRD patterns of Cu(II)-exchanged zeolites (λ=1.5418 Å) *The additional peaks at the 2θ of 15.8° and 26. 1° indicate presence of an extra analcime (ANA) phase

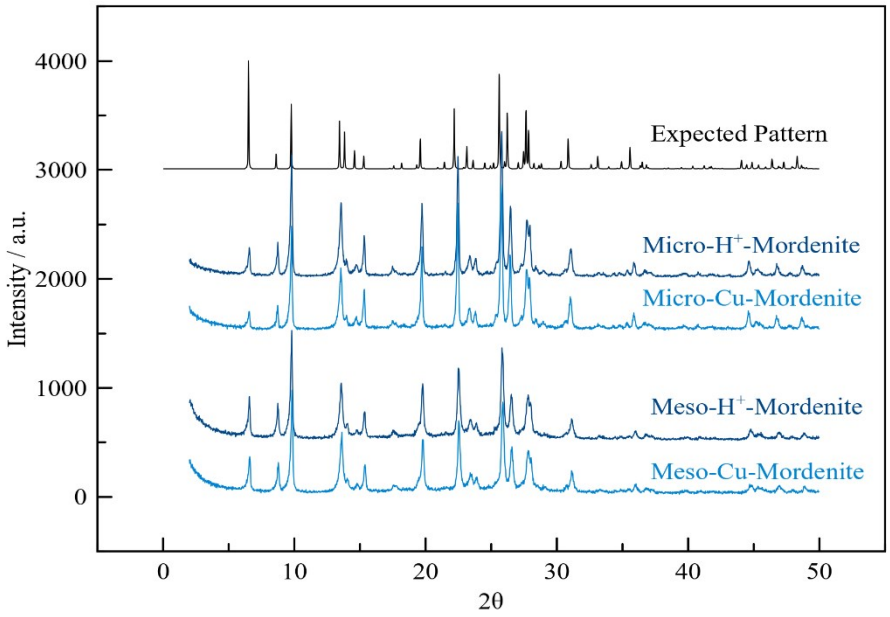

Fig. S2. Powder XRD patterns of commercial Mordenite and mesoporous Mordenite following Cu-exchange (λ=1.5418 Å).

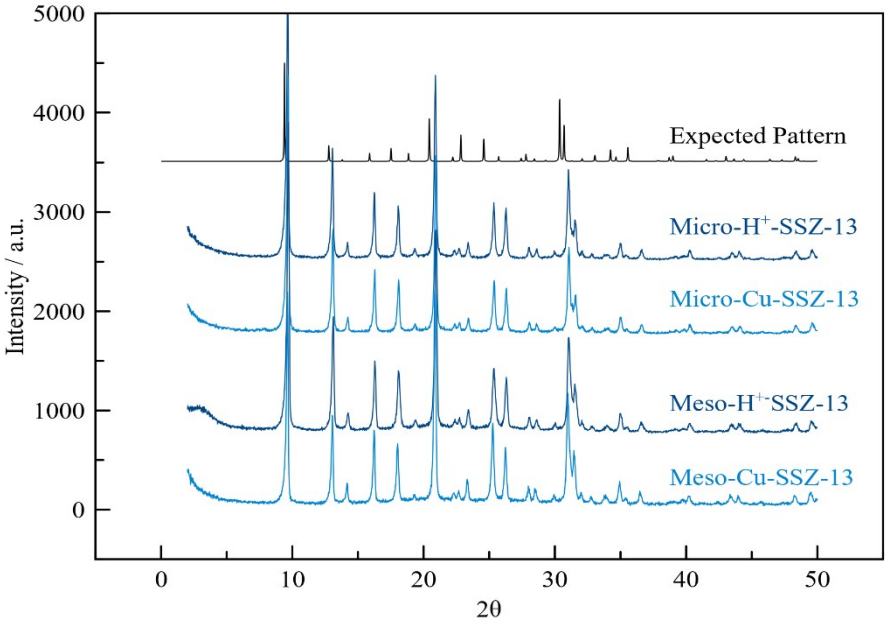

Fig. S3. Powder XRD patterns of calcined SSZ-13 and mesoporous SSZ-13 following Cu-exchange (λ=1.5418 Å). Expected pattern has different unit cell length due to the difference in Si/Al ratio. (Expected pattern has Si/Al=2.15)

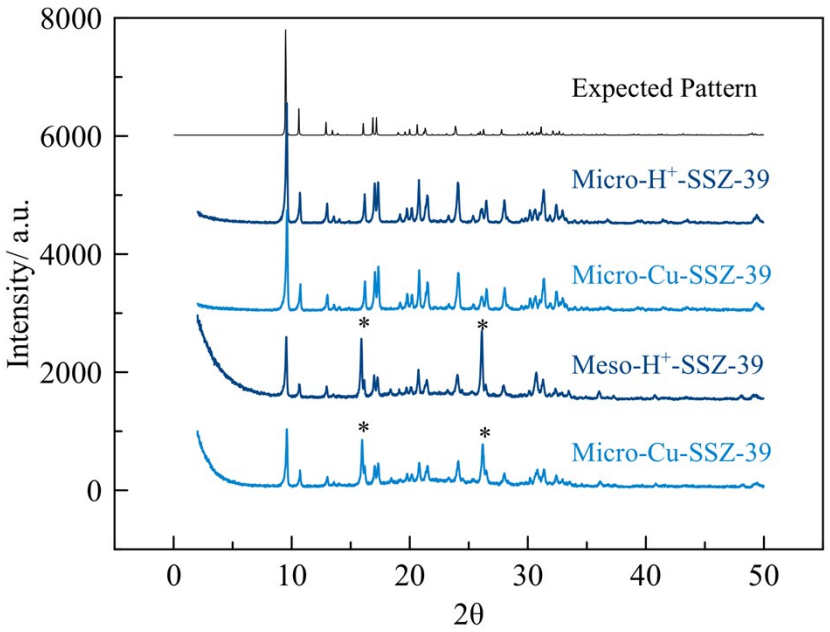

Fig. S4. Powder XRD patterns of calcined SSZ-39 and mesoporous SSZ-39 following Cu-exchange (λ=1.5418 Å). The additional peaks at the 2θ of 15.8° and 26. 1° (marked by an asterisk) indicate presence of an extra analcime (ANA) phase

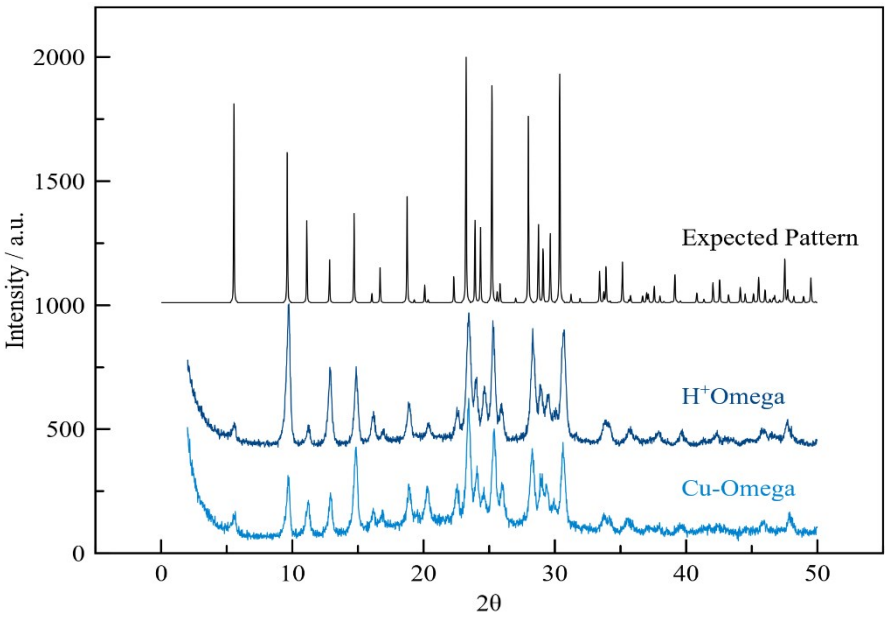

Fig. S5. Powder XRD patterns of calcined Omega following Cu-exchange (λ=1.5418 Å).

S2.2. Elemental Analysis

Table S2. Elemental composition for microporous and mesoporous/microporous Cu-zeolites

	Si/Al	Cu/Al	Cu concentration/ mmol g^{-1}
Micro-Cu-Mordenite	8.9±0.7	0.15±0.02	0.249
Meso-Cu-Mordenite	20±2	0.27±0.03	0.211
Micro-Cu-SSZ-13	9.7±0.8	0.10±0.01	0.154
Micro-Cu-SSZ-13-2	10.2±0.3	0.31±0.01	0.448
Meso-Cu-SSZ-13	14±2	0.32±0.05	0.348
Micro-Cu-SSZ-39	6.3±0.4	0.22±0.04	0.487
Micro-Cu-SSZ-39-2	7.0±0.5	0.33±0.01	0.660
Meso-Cu-SSZ-39	15±2	0.29±0.06	0.296
Cu-Omega	3.1±0.1	0.12±0.01	0.490

S2.3. SEM Images

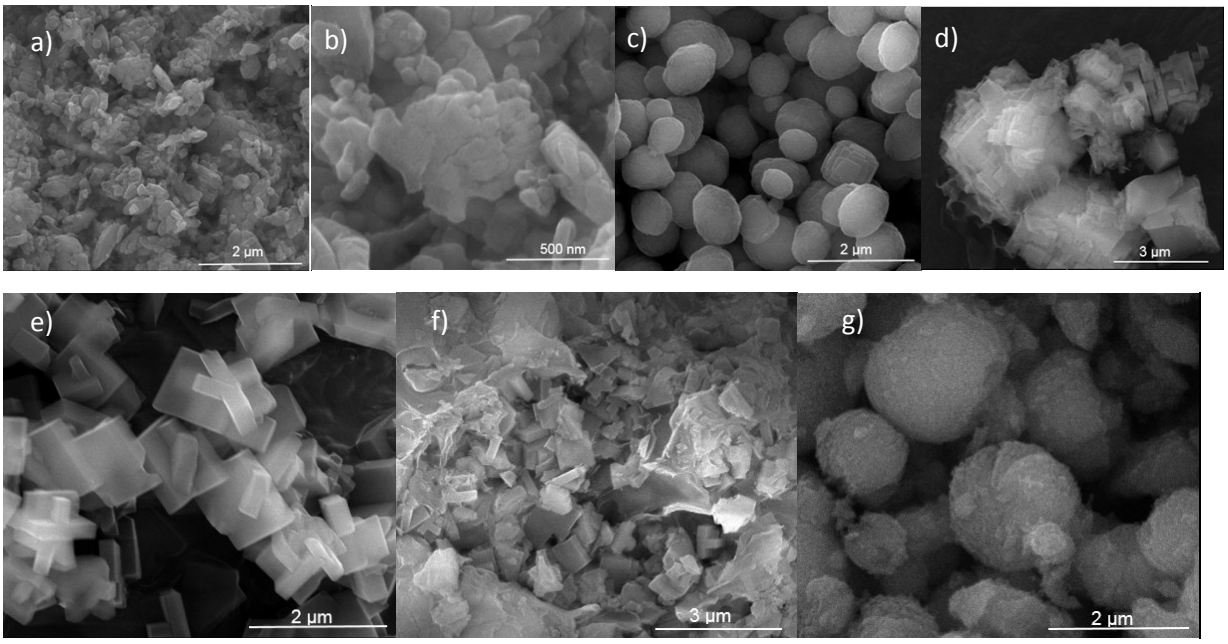

Fig. S6. SEM images of a) Micro-Cu-Mordenite, b) Meso-Cu-Mordenite, c) Micro-Cu-SSZ-13, d) Meso-Cu-SSZ-13. e) Micro-Cu-SSZ-39, f) Meso-Cu-SSZ-39 and g) Cu-Omega

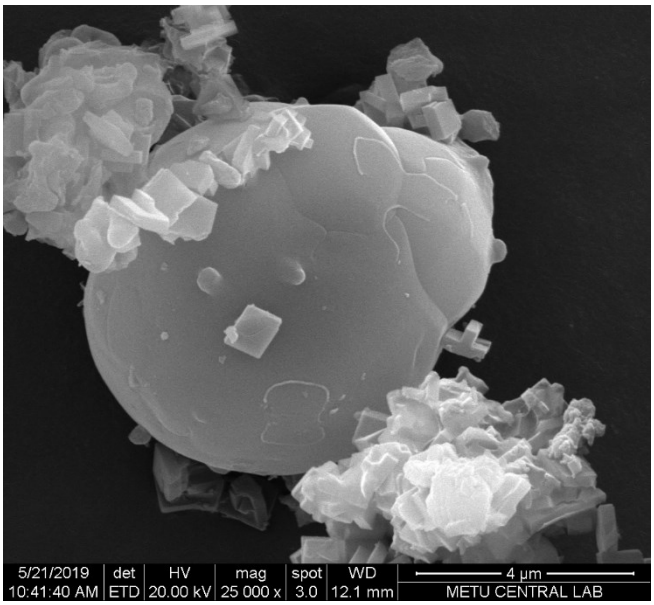

Fig. S7. SEM image of the analcime phase in Meso-Cu-SSZ-39

S2.4. Textural Properties

N_2 Adsorption Isotherms at 77 K

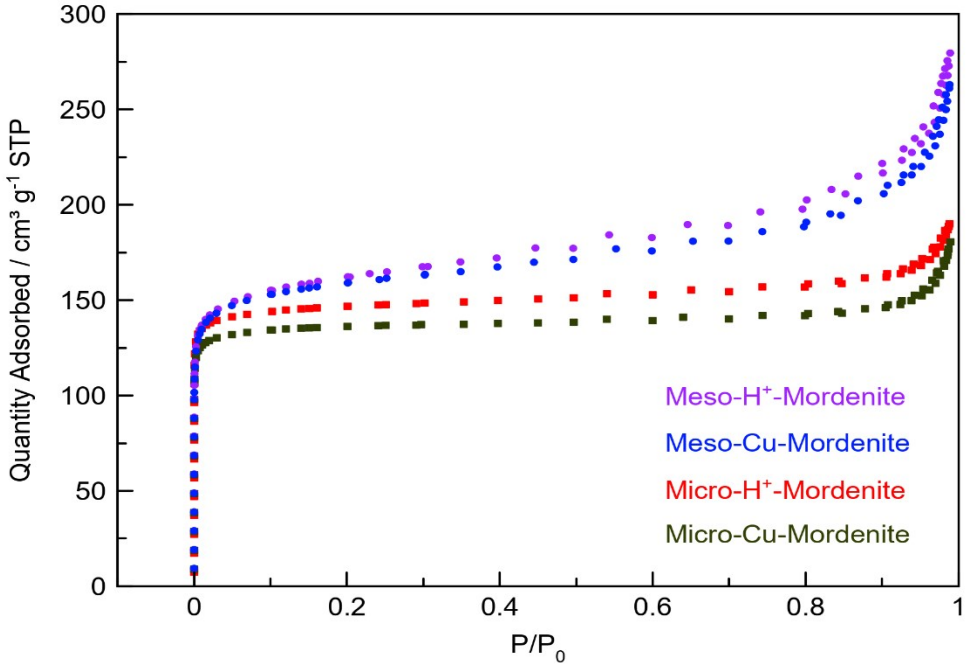

Fig. S8. N_2 adsorption/ desorption isotherms of micro- and mesoporous H^+- and Cu-Mordenite samples at 77 K

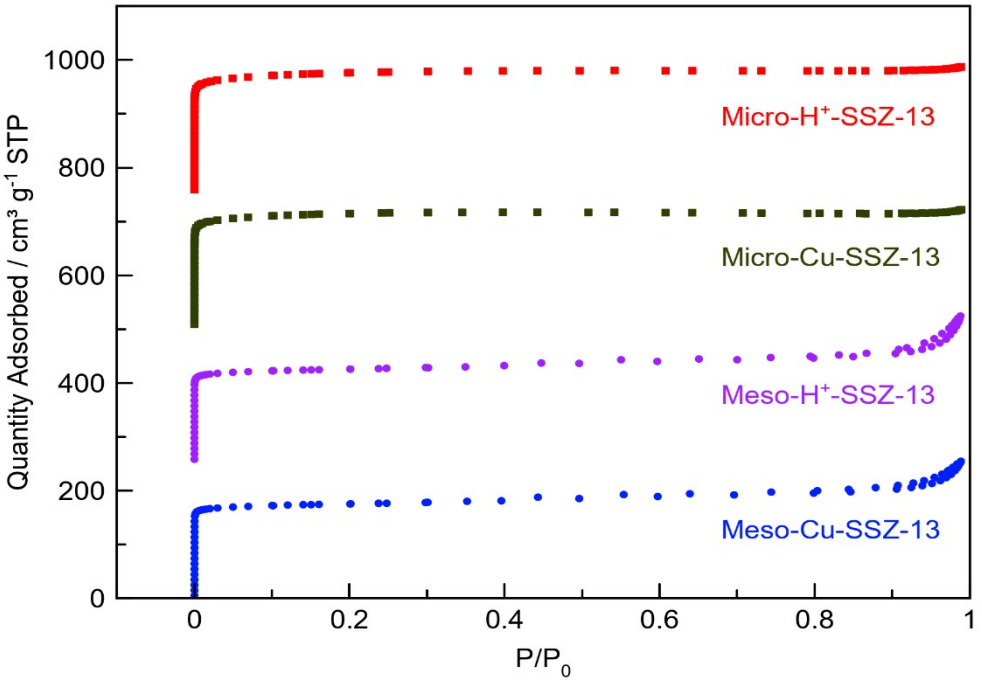

Fig. S9. N_2 adsorption/ desorption isotherms of micro- and mesoporous H^+- and Cu-SSZ-13 samples at 77 K

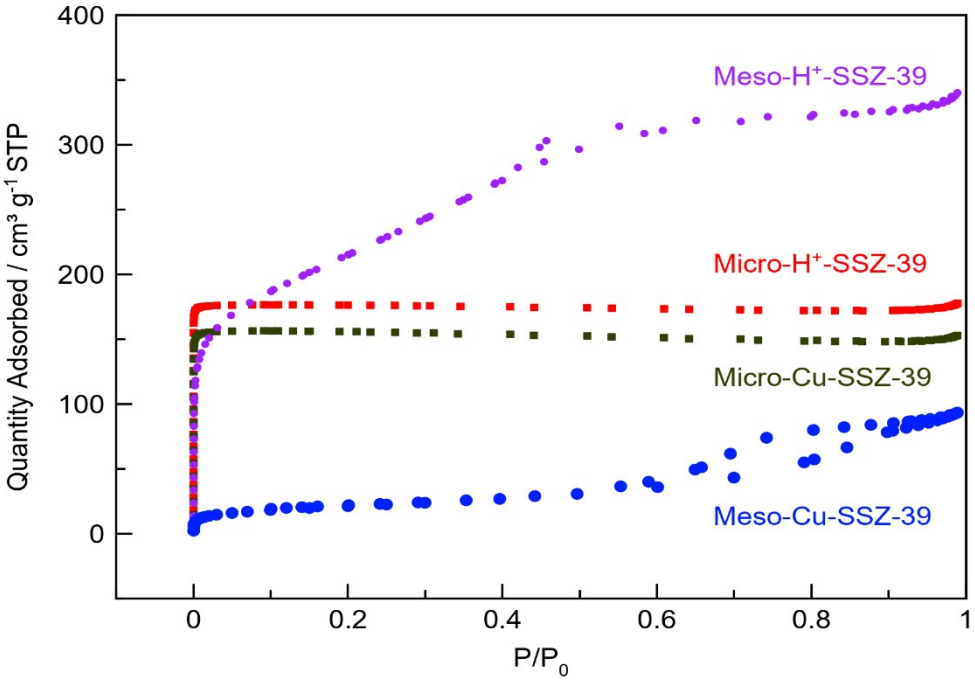

Fig. S10. N_2 adsorption/ desorption isotherms of micro- and mesoporous H^+- and Cu-SSZ-39 samples at 77 K

Table S3. Surface area and pore volume values of micro- and mesoporous H^+- and Cu(II)-exchanged zeolites

Zeolite	$S_{Langmuir}$ / $m^2\ g^{-1}$	S_{BET} / $m^2\ g^{-1}$	V_{total} / $cm^3\ g^{-1}$	V_{micro} [a] / $cm^3\ g^{-1}$	V_{meso} [b] / $cm^3\ g^{-1}$
Micro- H^+ Mordenite	473	645	0.285	0.202	0.083
Micro-Cu-Mordenite	440	597	0.264	0.193	0.071
Meso- H^+-Mordenite	421	575	0.361	0.163	0.191
Meso-Cu-Mordenite	519	709	0.386	0.189	0.197
Micro- H^+-SSZ-13	730	995	0.364	0.306	0.058
Micro-Cu-SSZ-13	692	943	0.340	0.294	0.046
Meso- H^+-SSZ-13	570	774	0.395	0.240	0.155
Meso-Cu-SSZ-13	568	771	0.374	0.241	0.133
Micro- H^+-SSZ-39	559	766	0.276	0.278	-
Micro-Cu-SSZ-39	490	676	0.247	0.247	-
Meso- H^+-SSZ-39	800	1099	0.557	0.056	0.501
Meso-Cu-SSZ-39	74	102	0.142	0.004	0.138
Na-Omega	206	151	0.161	0.050	0.111
Cu-Omega	347	254	0.228	0.092	0.136

a: t-plot V_{micro} = Micropore volume calculated using t-plot method
b: V_{meso} = Mesopore volume calculated from V_{total}- t-plot V_{micro}

Pore Size Distributions

The mesopore size distributions were estimated by using the Barrett– Joyner–Halenda (BJH) method from the desorption branch of the isotherms given in Fig. S9–S11. Both mesopore and macropore (> 50 nm) formation was observed in Meso-Mordenite and Meso-SSZ-13 samples; whereas mesopores in the range of ~ 2–5 nm, and in the range of ~ 5–10 nm were observed for Meso-Cu-SSZ-39 and Cu-Omega.

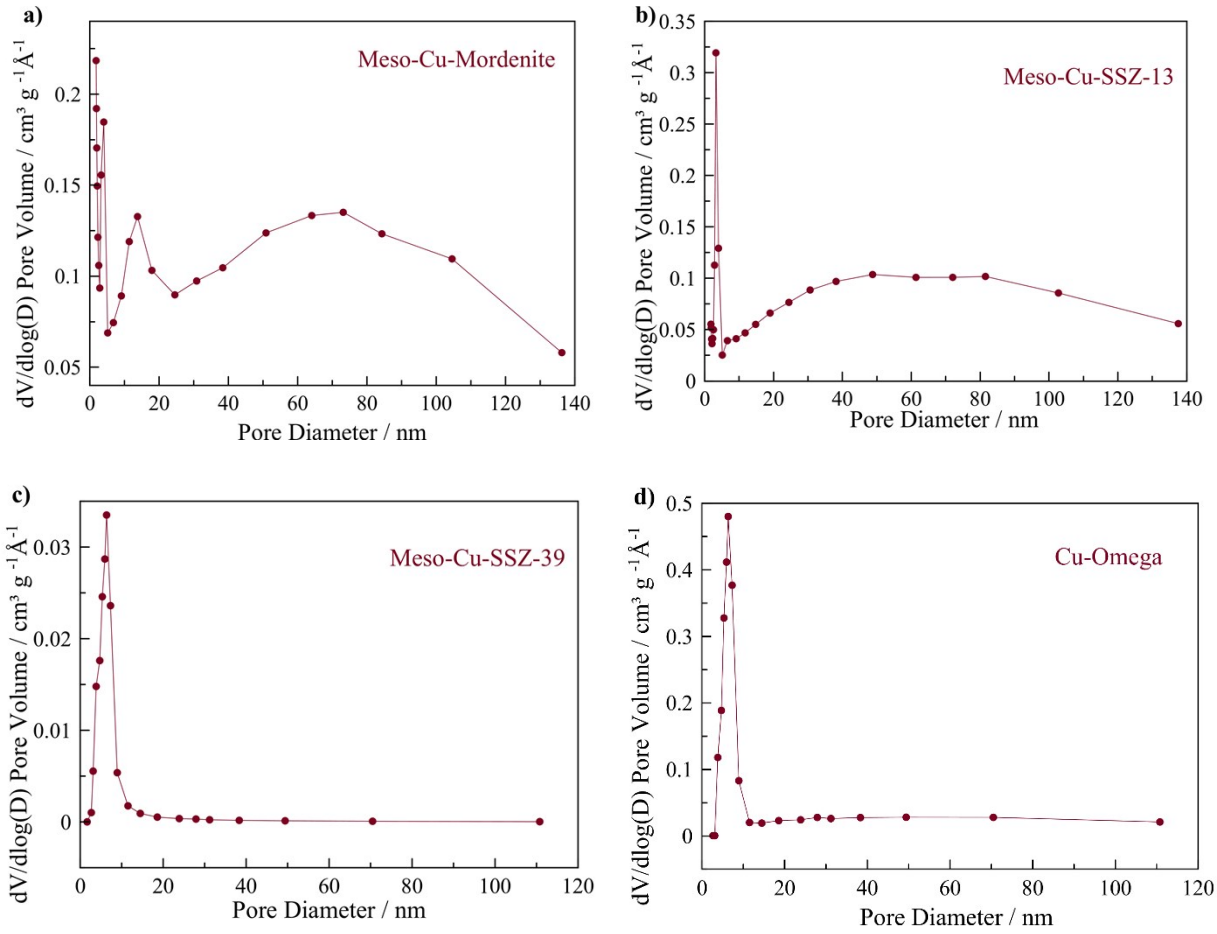

Fig. S11. Pore size distribution of a)Meso-Cu-Mordenite, b) Meso-Cu-SSZ-13, c) Meso-Cu-SSZ-39, d) Cu-Omega calculated using BJH model from desorption branch

S2.5. MAS NMR Analysis

^{27}Al MAS NMR was carried out with Bruker Superconducting FT.NMR Spectrometer Avance TM 300 MHz WB operating at B0=7T and SFO1=78.120739 MHz (transmitter frequency) equipped with Bruker 4 mm MAS probe 1H/BB. Samples were spun at 8500 Hz. FID is collected with D1=1s (relaxation delay), DW=5us (Dwell time), DE=6us (pre-scan delay) p1=3.86us (high power pulse) and PL1=120dB (power level for pulse).

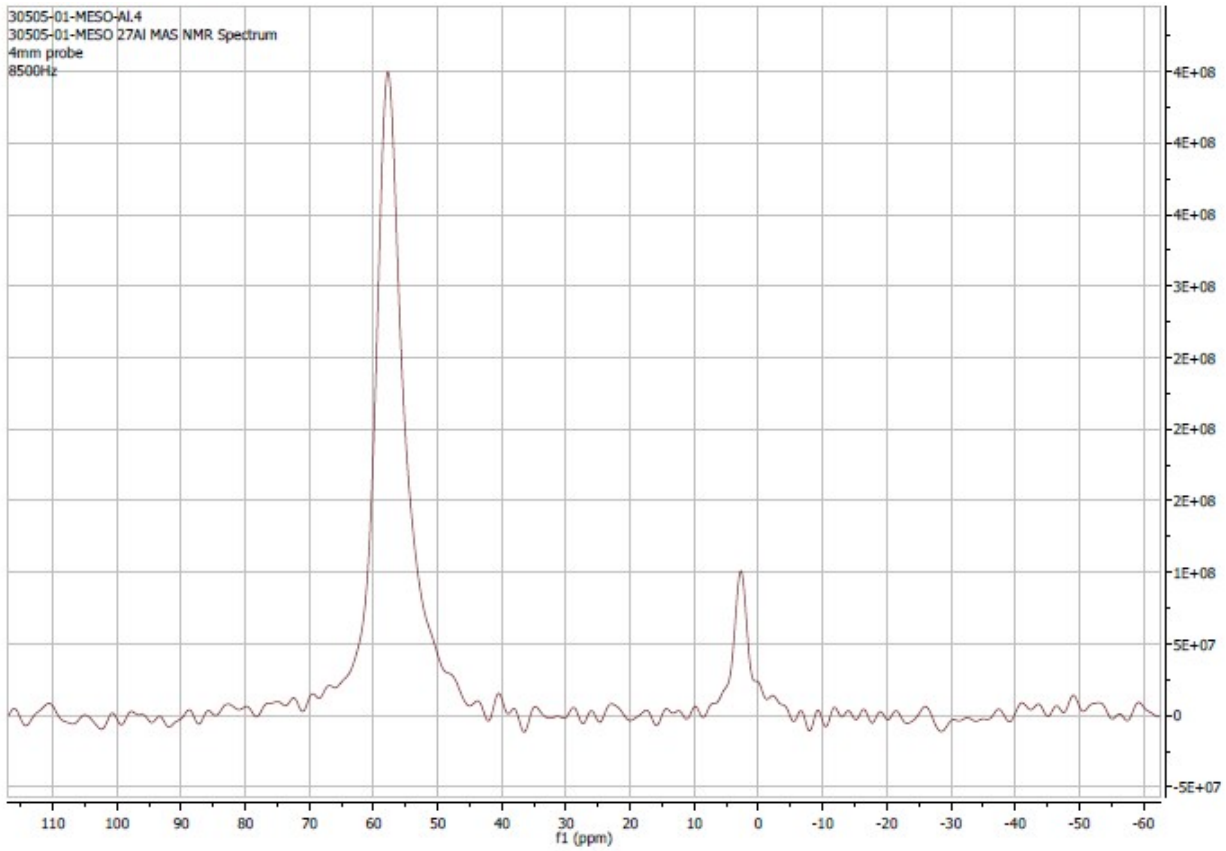

Fig. S12 ^{27}Al MAS NMR of Meso-Mordenite

S3. Reaction Results

Table S4. Methane conversion to methanol reaction results on Micro-Cu-SSZ-39 (Si/Al = 6.3, Cu/Al = 0.22) obtained at 573 K and 20.3 –40.5 kPa CH_4, 5.1–20.3 kPa N_2O, 2.6 kPa H_2O, balance He (~300 mg catalyst, 100 sccm total flow, GHSV= 10400 h^{-1})

P_{CH4}/ kPa	P_{N2O} / kPa	r_{CH3OH} / µmol g^{-1} h^{-1}	r_{DME} / µmol g^{-1} h^{-1}	r_{CO2} / µmol g^{-1} h^{-1}	r_{CO} / µmol g^{-1} h^{-1}	r_{CH4} / µmol g^{-1} h^{-1}	CH_4 Conversion / %	N_2O Conversion / %	TOF CH_4 / h^{-1}	TOF CH_3OH / h^{-1}	S_{CH3OH} / %
40.5	5.1	56±1	2.2±0.1	6±1	62±5	128	0.036	0.28	0.26	0.12	44
40.5	10.1	90±1	5.6±0.1	13±1	103±5	218	0.061	0.25	0.45	0.19	41
40.5	15.2	110±2	8.3±0.2	19±1	115±9	259	0.075	0.22	0.53	0.22	42
40.5	20.3	127±7	10.8±0.1	24±2	137±30	309	0.087	0.21	0.63	0.26	41
20.3	10.1	58.5±0.4	2±0.1	10±1	18±5	90.5	0.043	0.17	0.19	0.12	64
30.4	10.1	85.7±1.5	3.8±0.3	7.3±1	45±5	145.5	0.047	0.20	0.30	0.18	59
40.5	10.1	90.6±0.7	5.4±0.1	14.9±0.5	90±9	206.5	0.050	0.22	0.42	0.19	44

Table S5. Methane conversion to methanol reaction results on Micro-Cu-SSZ-39 (Si/Al = 6.3, Cu/Al = 0.22) obtained at 598 K and 70.9 kPa CH_4, 5.1–20.3 kPa N_2O, 2.6 kPa H_2O, balance He (~300 mg catalyst, 100 sccm total flow, GHSV= 10400 h^{-1})

P_{CH4}/ kPa	P_{N2O} / kPa	r_{CH3OH} / µmol g^{-1} h^{-1}	r_{DME} / µmol g^{-1} h^{-1}	r_{CO2} / µmol g^{-1} h^{-1}	r_{CO} / µmol g^{-1} h^{-1}	r_{CH4} / µmol g^{-1} h^{-1}	CH_4 Conversion / %	N_2O Conversion / %	TOF CH_4 / h^{-1}	TOF CH_3OH / h^{-1}	S_{CH3OH} / %
70.9	5.1	176±4	21±1	30±1	191±22	439	0.074	1.1	0.90	0.36	40
70.9	10.1	245±5	37±2	55±4	300±48	676	0.116	0.94	0.45	0.50	36
70.9	15.2	315±4	58±2	107±2	426±0	964	0.160	0.88	0.53	0.64	33
70.9	20.3	347±8	71±3	107±4	593±24	1188	0.200	0.77	0.63	0.71	29

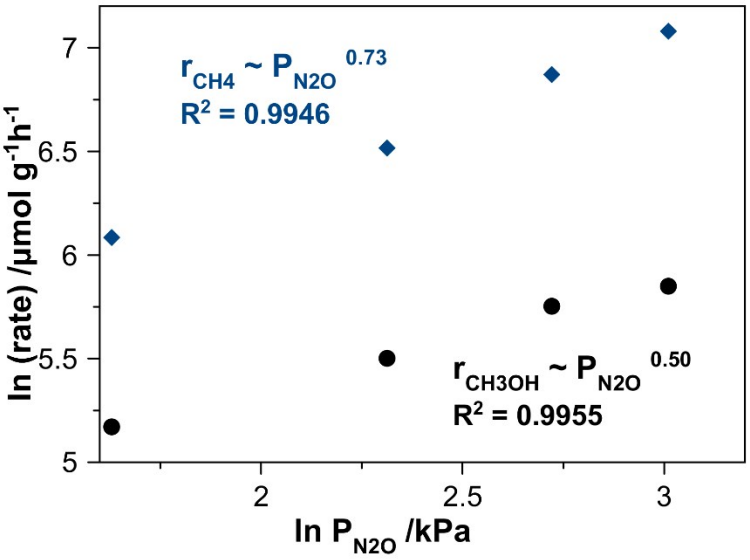

Fig. S13.ln (r_{CH4}) and ln (r_{CH3OH}) vs. ln(P_{N2O}) graphs on Micro-Cu-SSZ-39 (Si/Al = 6.3, Cu/Al = 0.22) obtained at 598 K and 70.9 kPa CH_4, 5.1–20.3 kPa N_2O, 2.6 kPa H_2O, balance He, (~300 mg catalyst, 100 sccm total flow, GHSV= 10400 h^{-1})

Table S6. Methane conversion to methanol reaction results on Micro-Cu-SSZ-39 (Si/Al = 6.3, Cu/Al = 0.22) and Micro-Cu-SSZ-39 (Si/Al = 7, Cu/Al = 0.33) obtained at 598 K and 40.5 kPa CH_4, 15.2 kPa N_2O, 2.6–10.1 kPa H_2O, balance He (~300 mg catalyst, 100 sccm total flow, GHSV= 10400 h^{-1})

Sample	**P_{H2O} / kPa**	**r_{CH3OH} / µmol g^{-1} h^{-1}**	**r_{DME} / µmol g^{-1} h^{-1}**	**r_{CO2} / µmol g^{-1} h^{-1}**	**r_{CO} / µmol g^{-1} h^{-1}**	**r_{CH4} / µmol g^{-1} h^{-1}**	**CH_4 Conversion / %**	**N_2O Conversion / %**	**TOF CH_4 / h^{-1}**	**TOF CH_3OH / h^{-1}**	**S_{CH3OH} / %**
Micro-Cu-SSZ-39	2.6	329±8	40±2	34±1	445±29	888	0.20	0.53	1.82	0.68	37
Micro-Cu-SSZ-39	3.8	463±8	50±1	44±5	610±17	1216	0.23	0.58	2.50	0.95	38
Micro-Cu-SSZ-39	4.0	499±4	57±2	110±10	728±27	1451	0.28	0.74	2.98	1.02	34
Micro-Cu-SSZ-39	10	311±14	19±3	90±4	336±23	773	0.15	0.39	1.58	0.63	40
Micro-Cu-SSZ-39-2	4.0	76±1	2.3±0.1	94±4	238±21	413	0.12	0.42	0.63	0.12	18

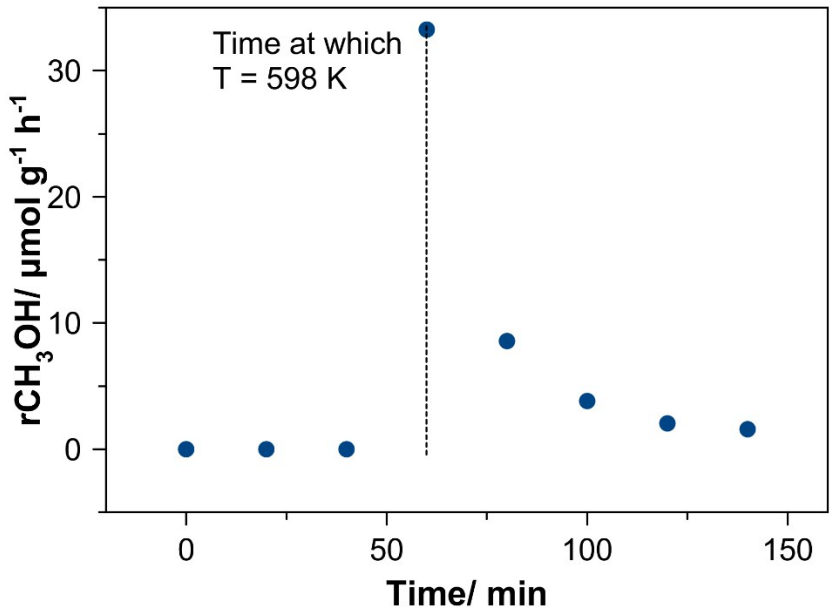

Fig. S14. Rate of methanol formation with respect to time on Micro-Cu-SSZ-39 (Si/Al = 6.3, Cu/Al = 0.22) obtained at 598 K and 40.5 kPa CH_4, 0 kPa N_2O, 2.6 kPa H_2O, balance He (~300 mg catalyst, 100 sccm total flow, GHSV= 10400 h^{-1})

Table S7. Methane conversion to methanol reaction results on Micro-Cu-SSZ-39 (Si/Al = 6.3, Cu/Al = 0.22) obtained at 543–598 K and 40.5 kPa CH_4, 15.2 kPa N_2O, 2.6 kPa H_2O, balance He (~300 mg catalyst, 100 sccm total flow, GHSV= 10400 h^{-1})

Temperature/ K	**r_{CH3OH} / µmol g^{-1} h^{-1}**	**r_{DME} / µmol g^{-1} h^{-1}**	**r_{CO2} / µmol g^{-1} h^{-1}**	**r_{CO} / µmol g^{-1} h^{-1}**	**r_{CH4} / µmol g^{-1} h^{-1}**	**CH_4 Conversion / %**	**N_2O Conversion / %**	**TOF CH_4 / h^{-1}**	**TOF CH_3OH / h^{-1}**	**S_{CH3OH} / %**
543	22±2	0.4±0.1	5±1	27±5	54.6	0.01	0.04	0.11	0.05	41
573	110±2	8.3±0.2	19±1	115±9	259	0.08	0.22	0.53	0.22	42
598	329±8	40±2	34±1	445±29	888	0.20	0.53	1.82	0.67	37

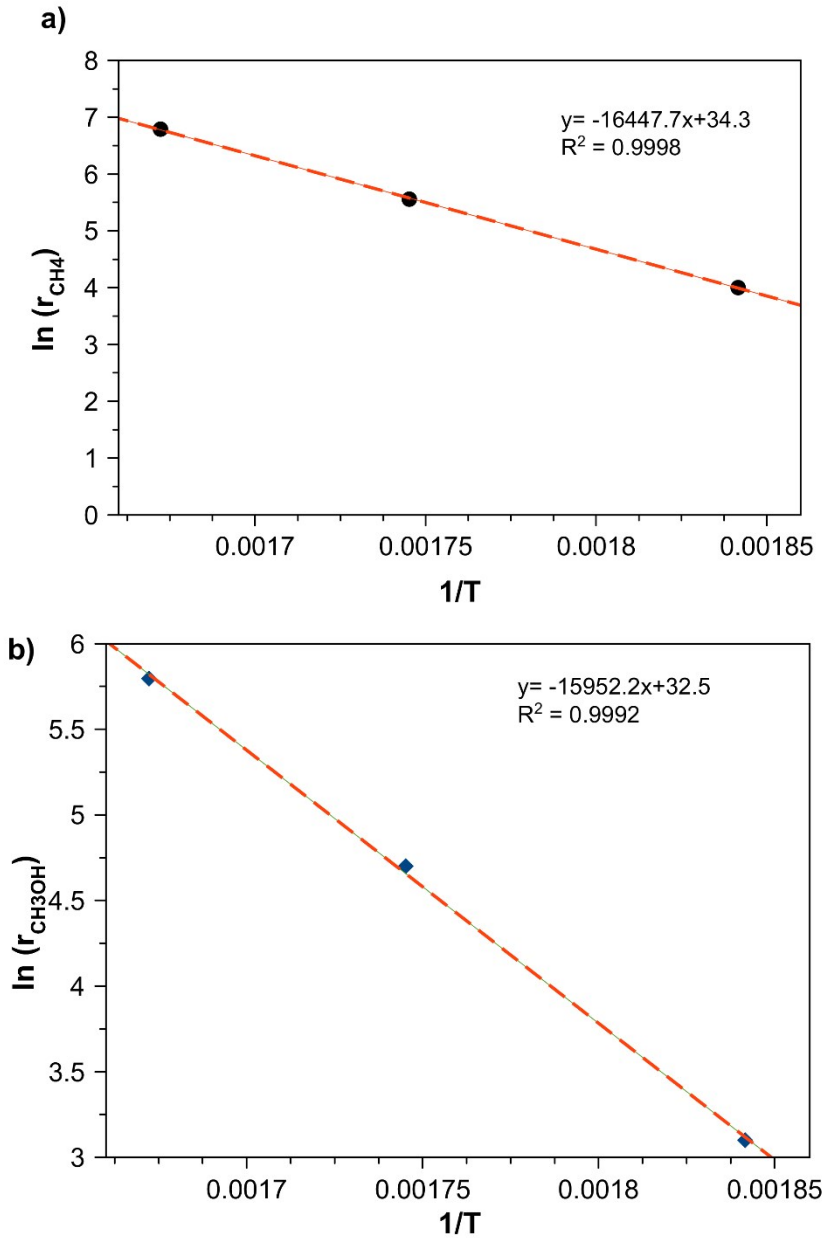

Fig. S14. a) ln (r_{CH4}) and b) ln (r_{CH3OH}) vs. 1/T graphs for activation energy calculations on Micro-Cu-SSZ-3

References

1 B. Ipek, M. J. Wulfers, H. Kim, F. Göltl, I. Hermans, J. P. Smith, K. S. Booksh, C. M. Brown and R. F. Lobo, *ACS Catal.*, 2017, **7**, 4291–4303.

2 A. M. Goossens, E. J. P. Feijen, G. Verhoeven, B. H. Wouters, P. J. Grobet, P. A. Jacobs and J. A. Martens, *Microporous Mesoporous Mater.*, 2000, **35–36**, 555–572.

3 G. Li, P. Vassilev, M. Sanchez-Sanchez, J. A. Lercher, E. J. M. Hensen and E. A. Pidko, *J. Catal.*, 2016, **338**, 305–312.

4 K. Leng, Y. Sun, X. Zhang, M. Yu and W. Xu, *Fuel*, 2016, **174**, 9–16.

5 A. Galarneau, J. Rodriguez and B. Coasne, , DOI:10.1021/la5026679.

6 E. P. Barrett, L. G. Joyner and P. P. Halenda, *J. Am. Chem. Soc.*, 1951, **73**, 373–380.